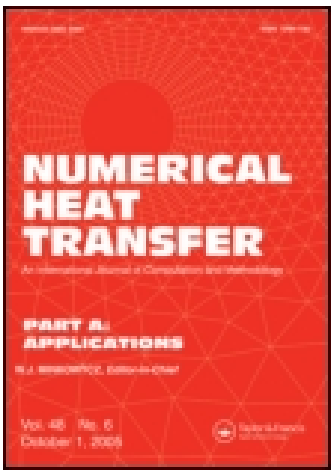

Numerical Heat Transfer, Part A: Applications: An International Journal of Computation and Methodology

Publication details, including instructions for authors and subscription information:
http://www.tandfonline.com/loi/unht20

NUMERICAL SIMULATIONS OF PARTICLE-LADEN AXISYMMETRIC TURBULENT FLOWS

S. Liao, F. M Ashayek, D. Guo
Published online: 15 Dec 2010.

To cite this article: S. Liao, F. M Ashayek, D. Guo (2001) NUMERICAL SIMULATIONS OF PARTICLE-LADEN AXISYMMETRIC TURBULENT FLOWS, Numerical Heat Transfer, Part A: Applications: An International Journal of Computation and Methodology, 39:8, 847-855, DOI: 10.1080/10407780120257

To link to this article: http://dx.doi.org/10.1080/10407780120257

Numerical Heat Transfer, Part A, 39:847–855, 2001

1040-7782/01 $12.00 + .00

TECHNICAL NOTE

NUMERICAL SIMULATIONS OF PARTICLE-LADEN AXISYMMETRIC TURBULENT FLOWS

S. Liao
School of Naval Architecture and Ocean Engineering, Shanghai Jiao Tong University, Shanghai, China

F. Mashayek and D. Guo
Department of Mechanical Engineering, University of Illinois at Chicago, Chicago, Illinois, USA

INTRODUCTION

In this short communication, we report some of our recent results obtained from direct numerical simulation (DNS) of two homogeneous particle-laden turbulent flows, namely, axisymmetric contraction and expansion, which have been previously studied in the context of single-phase flows [1]. This work extends our previous efforts (see, e.g., [2] and references therein) in generating a reliable data bank for preliminary assessment of various statistical/stochastic models for particle-laden turbulent flows. Because of space limitation, we restrict the presentation of the results to only those statistics that are required in the process of model assessment [3–5].

For the incompressible, axisymmetric contraction and expansion flows considered in this study, the instantaneous velocity field can be described as

$$\hat{U}_\alpha = U_{\alpha,\alpha} x_\alpha + u_\alpha \qquad \alpha = 1, 2, 3 \tag{1}$$

with no summation over Greek indices. Here, the hat $\hat{}$ denotes the instantaneous quantity, u_α is the carrier-phase fluctuating velocity in the x_α direction, and $U_{\alpha,\alpha} = dU_\alpha/dx_\alpha$ where $U_\alpha = \langle \hat{U}_\alpha \rangle$ with $\langle\ \rangle$ denoting the Eulerian ensemble average over the number of grid points. The intensity (or rapidity) of a mean strain rate, referred to as "equivalent mean strain rate" [1], can be measured in terms of $S = (S_{ij}S_{ij}/2)^{1/2}$ where $S_{ij} = (U_{i,j} + U_{j,i})/2$ and summation over repeated indices

Received 28 November 2000; accepted 20 December 2000.

The support for this work was provided by the National Science Foundation and the Office of Naval Research under grants CTS-0096349 and N00014-01-1-0122. The computational resources were provided by the San Diego Supercomputing Center.

Address correspondence to Professor F. Mashayek, Department of Mechanical Engineering (MC 251), University of Illinois at Chicago, 842 W. Taylor Street, Chicago, IL 60607. E-mail: mashayek@uic.edu

is implied. For axisymmetric contraction and expansion flows, respectively, we have

$$S_{ij} = \frac{2S}{\sqrt{3}} \begin{pmatrix} +1 & 0 & 0 \\ 0 & -\frac{1}{2} & 0 \\ 0 & 0 & -\frac{1}{2} \end{pmatrix} \qquad S_{ij} = \frac{2S}{\sqrt{3}} \begin{pmatrix} -1 & 0 & 0 \\ 0 & +\frac{1}{2} & 0 \\ 0 & 0 & +\frac{1}{2} \end{pmatrix} \tag{2}$$

In the following, we present the formulation of the problem in a general manner that is also applicable to our previously studied plain strain flow [2], provided that the corresponding mean strain rate tensor, S_{ij}, is used.

FORMULATION AND METHODOLOGY

The carrier and dispersed phases are simulated in the Eulerian and Lagrangian frames, respectively. Let $\hat{P}$, $\hat{U}_i$,$\hat{V}_i$, and $\hat{U}_i^*$ denote the instantaneous fluid pressure, fluid velocity, particle velocity, and fluid velocity at the particle position X_i, respectively. The governing equations are described by the instantaneous continuity and momentum equations for the fluid:

$$\frac{\partial \hat{U}_j}{\partial x_j} = 0 \qquad \frac{\partial \hat{U}_i}{\partial t} + \frac{\partial (\hat{U}_i \hat{U}_j)}{\partial x_j} = -\frac{1}{\rho_f} \frac{\partial \hat{P}}{\partial x_i} + \nu \frac{\partial^2 \hat{U}_i}{\partial x_j \partial x_j} \tag{3}$$

along with the Lagrangian equations of motion for a single particle

$$\frac{dX_i}{dt} = \hat{V}_i \qquad \frac{d\hat{V}_i}{dt} = \frac{1}{\tau_p}(\hat{U}_i^* - \hat{V}_i) \tag{4}$$

where x_i and t are the spatial and temporal coordinates, ρ_f and ν denote the fluid density and kinematic viscosity, respectively, and the superscript * refers to a fluid property evaluated at the particle location. For a spherical particle, the particle time constant is defined as $\tau_p = \rho_p d_p^2/18\mu$, where ρ_p and d_p are the particle density and diameter, respectively, and $\mu = \rho_f \nu$. Here, we restrict our attention to small particles with $\rho_p \gg \rho_f$ such that only the Stokes drag (without a correction because of large particle Reynolds numbers) is required to describe the particle dynamics.

The main objective of the simulations is to furnish statistics of the fluctuating velocities for the assessment of statistical models. This requires the knowledge of the mean velocity of the dispersed phase (note that the mean velocity of the carrier phase is known a priori). Following the approach of Barré et al. [2], we provide analytical solutions for the mean velocity of the dispersed phase. We begin by ensemble averaging the particle momentum equation (3) (which, under the current conditions, also may be viewed as an Eulerian equation for the dispersed phase [6]):

$$\frac{D^V V_i}{Dt} = \left\langle\!\!\left\langle \frac{1}{\tau_p}(\hat{U}_i^* - \hat{V}_i) \right\rangle\!\!\right\rangle - \left\langle\!\!\left\langle v_j \frac{\partial v_i}{\partial x_j} \right\rangle\!\!\right\rangle \tag{5}$$

where $D^V/Dt = \partial/\partial t + V_j(\partial/\partial x_j)$, the notation $\langle\langle\ \rangle\rangle$ denotes the ensemble average associated with the dispersed phase, and $V_i\,(= \langle\langle \hat{V}_i \rangle\rangle)$ and v_i are the particle mean and fluctuating velocities, respectively. For a homogeneous dispersed phase, it can be shown that the last correlation in (5) vanishes [2]. Nevertheless, substituting (1) in (5) indicates that $V_i = U_i$ is *not* a solution for the particle mean velocity in the axisymmetric flows. Similar to Barré et al. [2], we consider only one-way

coupling and assume that the initial fluctuating velocity of the dispersed phase is isotropic. Then, in an analogous manner to that in [2], it can be shown that the particle mean velocity may be described as $V_\alpha = \sigma_\alpha(t)x_\alpha$, where

$$\sigma_\alpha(t) = \frac{(\xi_\alpha - V^0_{\alpha,\alpha})\eta_\alpha \exp(\eta_\alpha t) - (\eta_\alpha - V^0_{\alpha,\alpha})\xi_\alpha \exp(\xi_\alpha t)}{(\xi_\alpha - V^0_{\alpha,\alpha})\exp(\eta_\alpha t) - (\eta_\alpha - V^0_{\alpha,\alpha})\exp(\xi_\alpha t)} \tag{6}$$

$$\xi_\alpha = \frac{-1 + \sqrt{1 + 4U_{\alpha,\alpha}\tau_p}}{2\tau_p} \qquad \eta_\alpha = \frac{-1 - \sqrt{1 + 4U_{\alpha,\alpha}\tau_p}}{2\tau_p} \tag{7}$$

for $1 + 4U_{\alpha,\alpha}\tau_p > 0$,

$$\sigma_\alpha(t) = \frac{V^0_{\alpha,\alpha} - (V^0_{\alpha,\alpha} + 1/2\tau_p)t/2\tau_p}{1 + (V^0_{\alpha,\alpha} + 1/2\tau_p)t} \tag{8}$$

for $1 + 4U_{\alpha,\alpha}\tau_p = 0$, and

$$\sigma_\alpha(t) = \frac{2\omega\tau_p V^0_{\alpha,\alpha} - (V^0_{\alpha,\alpha} - 2U_{\alpha,\alpha})\tan(\omega t)}{2\omega\tau_p + (1 + 2\tau_p V^0_{\alpha,\alpha})\tan(\omega t)} \tag{9}$$

$$\omega = \frac{\sqrt{|1 + 4U_{\alpha,\alpha}\tau_p|}}{2\tau_p} \tag{10}$$

for $1 + 4U_{\alpha,\alpha}\tau_p < 0$. Here $V^0_{\alpha,\alpha}$ is the initial value of $\sigma_\alpha(t)$, and in our simulations we have used

$$V^0_{\alpha,\alpha} = \begin{cases} \dfrac{1}{2\tau_p}\left(-1 + \sqrt{1 + 4U_{\alpha,\alpha}\tau_p}\right) & \text{when } U_{\alpha,\alpha} \geq 0 \\ U_{\alpha,\alpha} & \text{otherwise} \end{cases} \tag{11}$$

It is emphasized that all of these expressions are valid for both axisymmetric contraction and expansion turbulent flows. They are also valid for the plain strain flow considered in [2].

The above discussion assumes the homogeneity of the flow, which is achieved through the coordinate transformation [1]:

$$\xi_i = B_{ij}(t)x_j \tag{12}$$

This transformation results in the following transport equation for the fluctuating velocity of the carrier phase:

$$\frac{\partial u_i}{\partial t} + U_{i,j}u_j + B_{mj}(t)\frac{\partial u_i u_j}{\partial \xi_m} + \frac{1}{\rho_f}B_{mi}(t)\frac{\partial p}{\partial \xi_m} = \nu B_{mj}(t)B_{nj}(t)\frac{\partial^2 u_i}{\partial \xi_m \partial \xi_n} \tag{13}$$

where

$$B_{ij}(t) = \begin{pmatrix} B^0_{11}\exp(-U_{1,1}t) & 0 & 0 \\ 0 & B^0_{22}\exp(-U_{2,2}t) & 0 \\ 0 & 0 & B^0_{33}\exp(-U_{3,3}t) \end{pmatrix} \tag{14}$$

for both contraction and expansion flows, with $B^0_{ij} = B_{ij}(0)$. Applying the

transformation to the particle momentum equation, we have

$$\frac{dv_i}{dt} = \frac{1}{\tau_p}(u_i^* - v_i) - V_{i,j}v_j \tag{15}$$

The right-hand side of this equation does not show any dependency on position. Therefore, if the initial particle fluctuating velocity is homogeneous, the evolution of v_i is independent of ξ_i and the turbulence remains homogeneous.

The numerical methodology is similar to that implemented in [2] and will not be repeated here for brevity. All the variables are normalized using reference scales for length (L_0), velocity (U_0), and density (ρ_0). The length scale is chosen, conveniently, such that the length of the computational domain is 2π and the carrier-phase density is taken as the reference density. The velocity scale is found by specifying a reference Reynolds number $\mathrm{Re}_0 = \rho_0 U_0 L_0/\mu = 232.6$, for all the simulations. The fluid fluctuating velocity u_i is calculated in the coordinate system $O - \xi_1\xi_2\xi_3$ and, with a priori knowledge of the mean velocity U_i, the instantaneous fluid velocity can be calculated using $\hat{U}_i = U_i + u_i$. The instantaneous particle velocity $\hat{V}_i$ is then directly obtained from solving Lagrangian particle equation (4) in the inertial coordinate system $O - x_1x_2x_3$ and the corresponding fluctuating particle velocity v_i is calculated using $v_i = \hat{V}_i - V_i$.

A Fourier pseudospectral method is employed for the spatial representation of the fluid pressure and fluctuating velocity in the $O - \xi_1\xi_2\xi_3$ coordinate system. All calculations for the carrier phase are performed in the Fourier space with the exception of the nonlinear terms. For the sake of aliasing errors, energies outside of a spherical wave number shell having radius $\sqrt{2}N/3$ are truncated, where N is the number of grid points in each direction. An explicit second-order accurate Adams–Bashford method is applied for the temporal advancement of both the Eulerian carrier phase equations and Lagrangian particle equations. A fourth-order accurate Lagrange polynomial interpolation scheme is applied to evaluate fluid variables at the particle locations. All the simulations are performed using $N = 128$ with a total number of particles $N_p = 1.2 \times 10^5$ and $\rho_p = 721.8$.

For all the simulations, the computational domain in the $O - \xi_1\xi_2\xi_3$ coordinate system is fixed in the region $[0, 2\pi] \times [0, 2\pi] \times [0, 2\pi]$. Nevertheless, according to (12) and (14), the corresponding physical domain in the $O - x_1x_2x_3$ coordinate system changes in time. If Γ_α denotes the length of the corresponding physical box in the x_α direction, then we have

$$\Gamma_\alpha(t) = \frac{2\pi}{B^0_{\alpha\alpha}}\exp(U_{\alpha,\alpha}t) \qquad \alpha = 1, 2, 3 \tag{16}$$

Thus, the length Γ_α in the x_α direction increases when $U_{\alpha,\alpha} > 0$ and decreases when $U_{\alpha,\alpha} < 0$. In other words, the corresponding physical domain is elongated (shortened) in the direction with positive (negative) mean strain rate. Therefore, if we begin with an isotropic mesh configuration with three identical sides in the physical coordinate system $O - x_1x_2x_3$, the mesh aspect ratio, defined as the ratio of the longest side of the mesh to the shortest side, increases in time. If the mesh aspect ratio becomes too large, it is difficult to resolve turbulence accurately in all directions. To allow the simulations to continue for a long time, we implement a predistorted initial physical domain with the short side in the direction to be

elongated by positive main strain rate and vice versa. For contraction flows, the initial mesh aspect ratio of the physical domain is $1/2 : \sqrt{2} : \sqrt{2}$ ($B^0_{11} : B^0_{22} : B^0_{33} = 2 : 1/\sqrt{2} : 1/\sqrt{2}$) and at the final simulation time it becomes $2 : 1/\sqrt{2} : 1/\sqrt{2}$ ($B_{11} : B_{22} : B_{33} = 1/2 : \sqrt{2} : \sqrt{2}$). For the expansion flows, the initial mesh aspect ratio of the physical domain is $2 : 1/\sqrt{2} : 1/\sqrt{2}$ ($B^0_{11} : B^0_{22} : B^0_{33} = 1/2 : \sqrt{2} : \sqrt{2}$) and this finally becomes $1/2 : \sqrt{2} : \sqrt{2}$ ($B_{11} : B_{22} : B_{33} = 2 : 1/\sqrt{2} : 1/\sqrt{2}$). All the simulations are stopped when the reference total strain $c = \exp(St)$ reaches 3.32.

The initial conditions for the axisymmetric flows are obtained by preliminary simulations of homogeneous decaying turbulence. In decaying simulations, the initial random velocity field for the carrier phase is given by the method described in [2]. Each simulation of decaying turbulence is performed on a domain described by the initial aspect ratio of the corresponding axisymmetric flow. This domain is kept the same throughout the decaying simulations, which are stopped once higher-order statistics reach their asymptotic values. Then, the results of the decaying simulations are used as the initial carrier-phase velocity for the axisymmetric flows. In the decaying cases, only the carrier phase is simulated. At the beginning of simulations of two-phase axisymmetric flows, the particles are randomly distributed throughout the corresponding physical domain and are specified to have no relative velocity with respect to the local fluid.

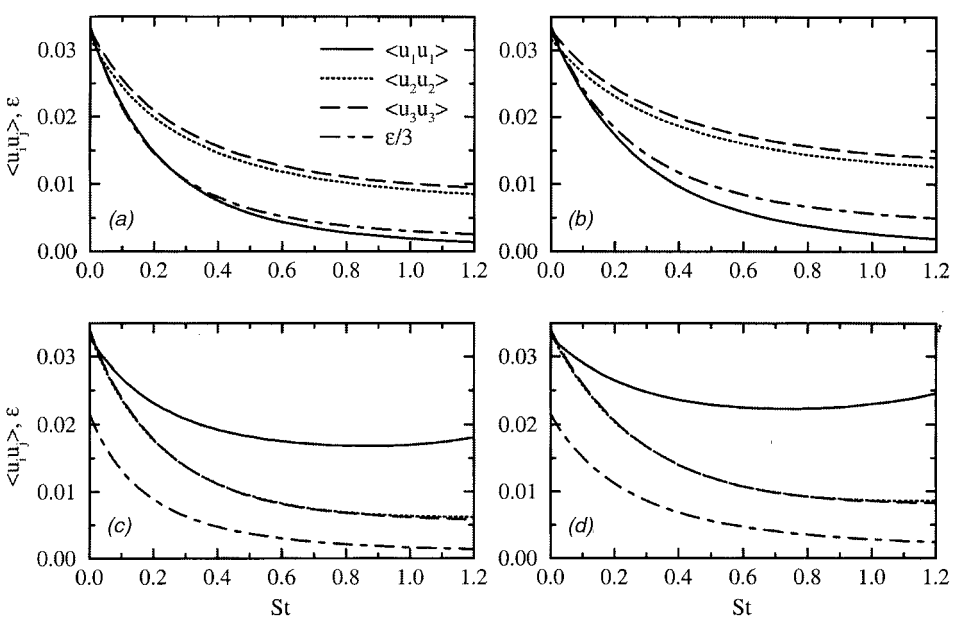

Figure 1. Temporal evolution of the carrier-phase Reynolds stress and dissipation rate for (*a*) contraction flow, $S = 0.619$; (*b*) contraction flow, $S = 0.866$; (*c*) expansion flow, $S = 0.385$; and (*d*) expansion flow, $S = 0.539$.

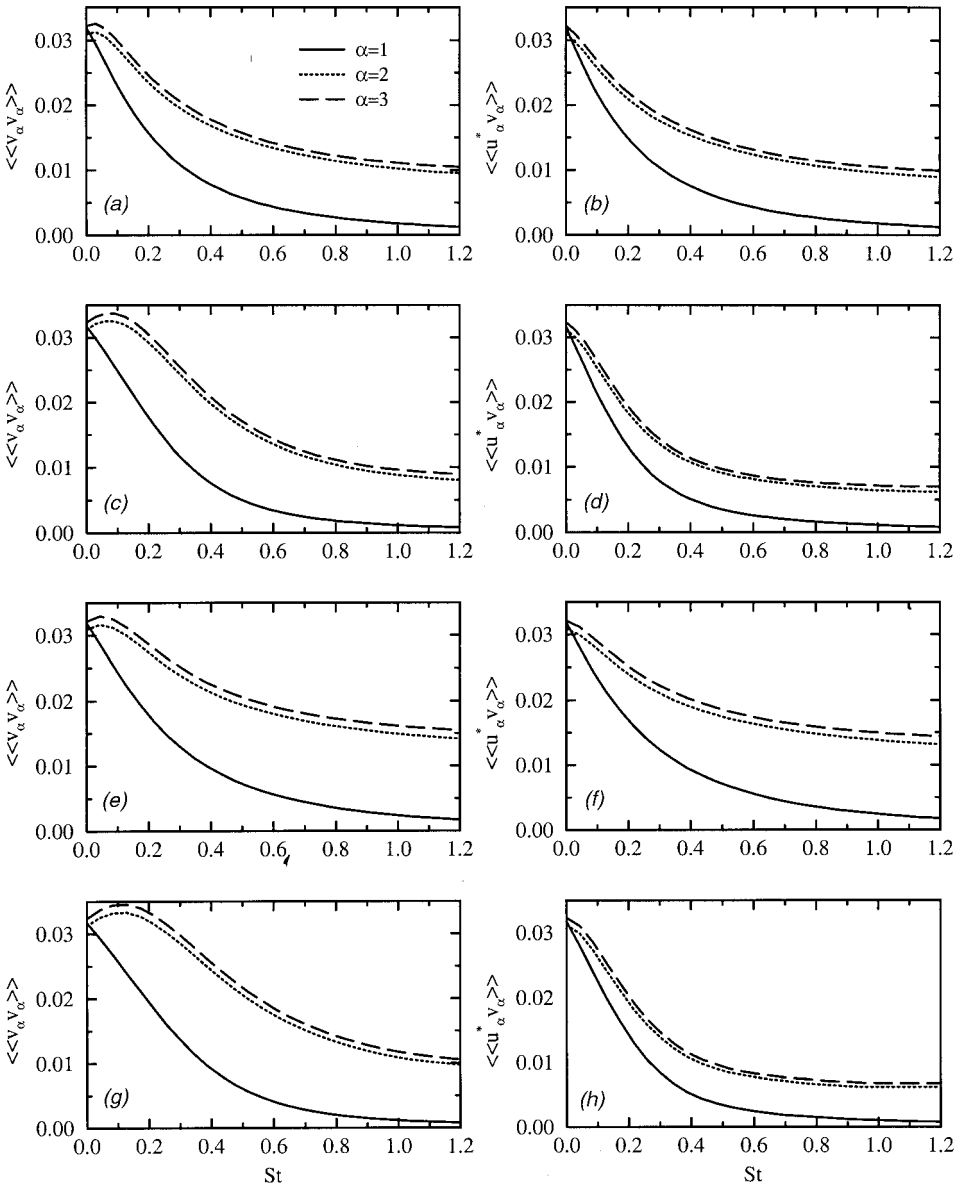

Figure 2. Temporal evolution of the dispersed-phase Reynolds stress and velocity covariance in the contraction flow. (*a*) and (*b*) $S = 0.619$, $\tau_p = 0.112$; (*c*) and (*d*) $S = 0.619$, $\tau_p = 0.434$; (*e*) and (*f*) $S = 0.866$, $\tau_p = 0.112$; (*g*) and (*h*) $S = 0.866$, $\tau_p = 0.434$.

RESULTS

The accuracy of the code has been checked using a variety of tests that are not included here for brevity. For each of the contraction or expansion flows, two dif-

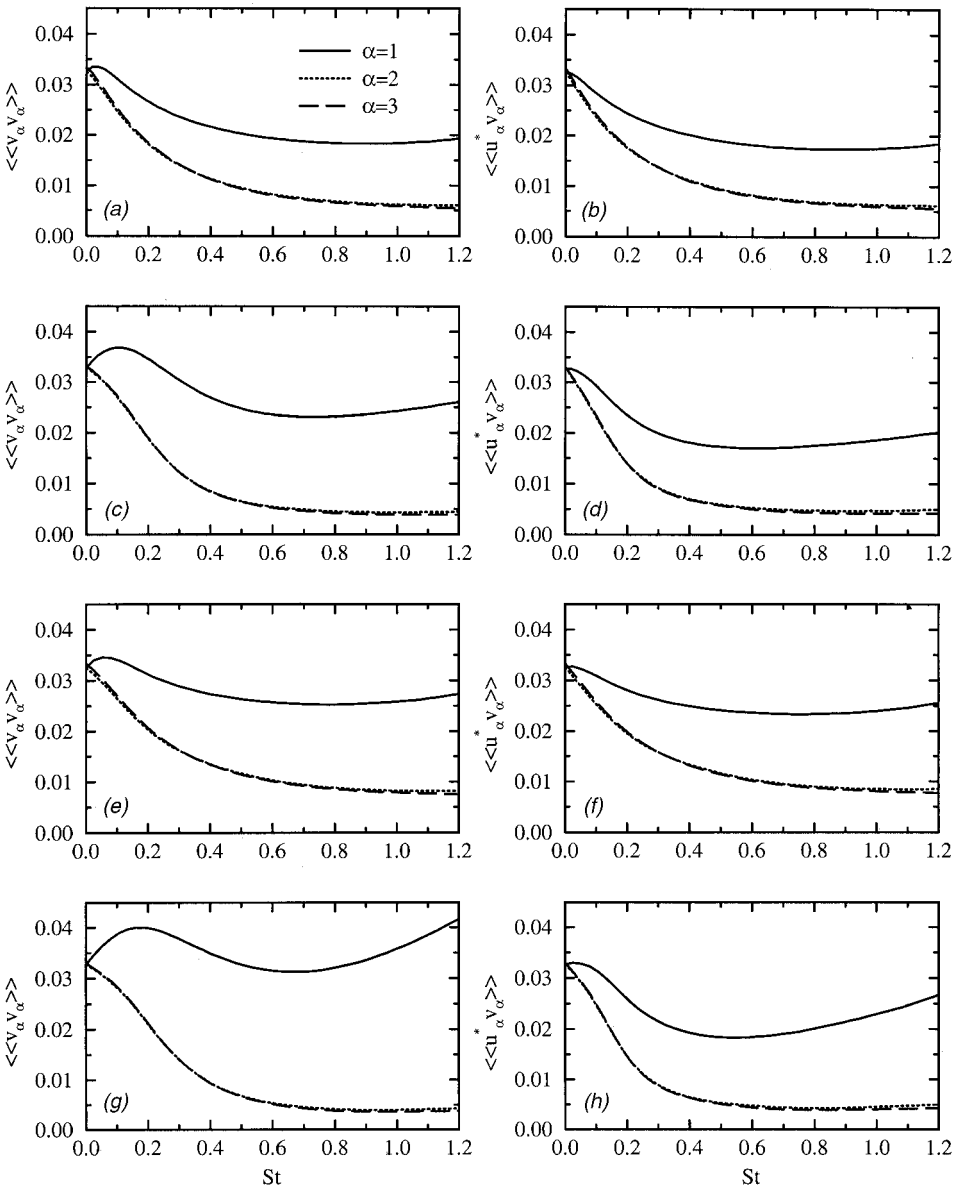

Figure 3. Temporal evolution of the dispersed-phase Reynolds stress and velocity covariance in the expansion flow. (*a*) and (*b*) $S = 0.385$, $\tau_p = 0.112$; (*c*) and (*d*) $S = 0.385$, $\tau_p = 0.434$; (*e*) and (*f*) $S = 0.539$, $\tau_p = 0.112$; (*g*) and (*h*) $S = 0.539$, $\tau_p = 0.434$.

ferent values of the normalized mean strain rate parameter $\tilde{S} = Sq^2/\varepsilon = 0.6$ and 0.84 are considered. Here, $q^2 = \langle u_i u_i \rangle$ is twice the turbulence kinetic energy and $\varepsilon = \nu \langle u_{i,j} u_{i,j} \rangle$ is the dissipation rate. Further, for a given mean strain rate parameter

$\tilde{S}$ of each kind of flow, two particle time constants ($\tau_p = 0.112$ and 0.434) are considered to investigate the effects of τ_p.

Because the main objective of this note is to provide statistics of two-phase flows for the assessment of various statistical/stochastic models, and also because of space limitation, here we present only our results for the fluid ($\langle u_i u_j \rangle$) and particle ($\langle\langle v_i v_j \rangle\rangle$) Reynolds stresses along with the velocity covariance $\langle\langle u_i^* v_j \rangle\rangle$. For the axisymmetric flows in which we are interested, all the shear components in these tensors are zero and we only present the temporal evolution of the normal components in Figures 1–3 for various cases. Included in Figure 1 is also the dissipation rate (ε) of the turbulence kinetic energy of the carrier phase, which is used (along with the turbulence kinetic energy) for the calculation of a turbulence time scale in most of the statistical models—it should be emphasized that the values of the dissipation rate shown on the figure are divided by 3 to allow their presentation within the scales used for the Reynolds stresses.

As we see in Figure 1, starting from the final output of the isotropic decaying simulations as the initial condition, all the axisymmetric flows initially experience a decay in Reynolds stresses and dissipation rate. Nevertheless, it is observed in expansion flows that the $\langle u_1 u_1 \rangle$ component starts to grow during the final stages of the simulations. This is attributed to the larger "negative" strain rate in this direction, which results in a stronger production term, that is, $\langle u_1 u_1 \rangle dU_1/dx_1$, in the transport equation for $\langle u_1 u_1 \rangle$. The increase in the production rate also explains the increase in all the Reynolds stresses in both flows, when a larger mean strain rate is applied. It should be mentioned that the small difference between $\langle u_2 u_2 \rangle$ and $\langle u_3 u_3 \rangle$ is an artifact of the slightly anisotropic initial conditions as produced numerically during the decaying simulations.

Similar features are observed for the temporal evolution of $\langle\langle v_i v_j \rangle\rangle$ and $\langle\langle u_i^* v_j \rangle\rangle$ in Figures 2 and 3. However, there is a notable initial increase in $\langle\langle v_i v_j \rangle\rangle$ in the directions with a positive rate of production, that is, the x_1 direction in the expansion flow and the x_2 and x_3 directions in the contraction flow. These values are also generally larger than their fluid counterparts, which is in agreement with previous studies in homogeneous shear and plane strain flows. It is clear that, because of the lack of a small-scale viscous dissipation, the particle Renolds stress components are able to grow as a result of the production by the mean velocity gradient. This is the phenomenon observed during the early stages; however, later the increase in the relative velocity between the particle and its surrounding fluid element enhances the dissipating effect of the drag. This finally causes the decrease in the particle Reynolds stresses in all directions. Based on our previous experience with statistical models, it appears that this behavior of the particle Reynolds stress creates one of the most stringent tests on the performance of the two-phase turbulence models.

REFERENCES

1. M. J. Lee and W. C. Reynolds, Numerical experiments on the structure of homogeneous turbulence, Department of Mechanical Engineering Report TF-24, Stanford University, Stanford, CA, 1985.

2. C. Barré, F. Mashayek, and D. B. Taulbee, Statistics in Particle-Laden Plane Strain Turbulence by Direct Numerical Simulation, *Int. J. Multiphase Flow*, vol. 27, no. 2, pp. 347–378, 2001.
3. L. I. Zaichik, A Statistical Model of Particle Transport and Heat Transfer in Turbulent Shear Flows, *Phys. Fluids*, vol. 11, no. 6, pp. 1521–1534, 1999.
4. K. E. Hyland, S. McKee, and M. W. Reeks, Exact Analytic Solutions to Turbulent Particle Flow Equations, *Phys. Fluids*, vol. 11, no. 5, pp. 1249–1261, 1999.
5. D. B. Taulbee, F. Mashayek, and C. Barré, Simulation and Reynolds Stress Modeling of Particle-Laden Turbulent Shear Flows, *Int. J. Heat Fluid Flows*, vol. 20, no. 4, pp. 368–373, 1999.
6. R. Jackson, Locally Averaged Equations of Motion for a Mixture of Identical Spherical Particles and a Newtonian Fluid, *Chem. Eng. Sci.*, vol. 52, no. 15, pp. 2457–2469, 1997.